CLOUDS, CRACKS AND FEM'S

J. TINSLEY ODEN*, and C. ARMANDO DUARTE†
Texas Inst. for Comput. and Appl. Math.
The University of Texas at Austin
Taylor Hall 2.400
Austin, Texas, 78712, U.S.A.

Dedicated to Professor John Martin on the Occasion of his Sixtieth Birthday

Abstract

This paper describes extensions of the *hp* cloud method to problems of fracture mechanics as an example of developing customized cloud functions. The cloud methods are built on partitions of unity that are subordinate to covers of the solution domain. For this reason, clouds can also be constructed on finite element meshes. This aspect of these methods is also discussed. Applications to representative boundary-value problems are presented.

1 Introduction

The notion of an *hp* cloud was introduced by the authors in 1995 [4] as a variant of the so-called meshless methods that began gaining interest around that time. These methods do not require the standard mesh connectivities of conventional finite elements and involve the construction of so-called *clouds*, which are overlapping open sets covering the domain of the solution of a boundary-value problem. A key feature of these sets of clouds is that they provide the domains of a partition of unity (PU),

*Professor, Director, TICAM. e-mail: oden@ticam.utexas.edu (corresponding author)
†Research Assistant, TICAM. e-mail: armando@ticam.utexas.edu

which is a set of functions with support contained in a cloud but whose values sum to the unity at each point $\boldsymbol{x}$ in the solution domain Ω.

An interesting and useful property of conventional finite element methods is that the usual FEM global basis functions N_α associated with nodes $\boldsymbol{x}_\alpha \in \Omega$ also form a PU since $\sum_\alpha N_\alpha(\boldsymbol{x}) = 1$. Thus FEM's can be used as a basis for clouds. While such an approach bypasses the advantages of some meshless methods, as one then has a FEM mesh, other useful properties are obtained, such as the ability to produce seamless *hp* FEM approximations with nonuniform h and p and the ease with which essential boundary conditions can be implemented on FEM meshes. An important feature of clouds and, especially of hybrid FEM-clouds, is the ability to develop customized clouds for specific applications. We exploit this feature in the present paper to develop clouds for problems of stress singularities and linear fracture mechanics.

The present paper is a summary and compilation of results developed by the authors in several recent papers. Our theory of clouds, presented in [2, 4], is summarized in Section 2, following this introduction. The use of FEM's to produce a PU, presented in [6], is briefly summarized in Section 2 as well. A detailed treatment, including studies of performance and adaptive *hp* cloud methods, is discussed in the thesis of C. A. Duarte [5] and in a forthcoming paper [3]. The use of customized clouds for singular problems was introduced in [7]; here we extend those results to plane elasticity problems with inclined cracks. The results of several numerical experiments are summarized in Section 3.

2 *Hp* Cloud Approximations, a Summary

In the *hp* cloud method introduced in [2, 4] the domain Ω of the solution of a boundary-value problem is covered with a finite open covering $\mathcal{T}_N := \{\omega_\alpha\}_{\alpha=1}^N$ consisting of N open sets ω_α (the *clouds*)

$$\bar{\Omega} \subset \bigcup_{\alpha=1}^{N} \bar{\omega}_\alpha \tag{1}$$

The center of the clouds, $\boldsymbol{x}_\alpha$, are denoted by *nodes*. The shape of a cloud ω_α can be quite arbitrary. In two dimensions, for example, it can be a rectangle, an ellipse or a circle. Figure 1 shows examples of valid open coverings and associated clouds.

The next step in building *hp* cloud approximations is to construct a partition of unity subordinated to the open covering $\mathcal{T}_N$. The partition of unity functions φ_α

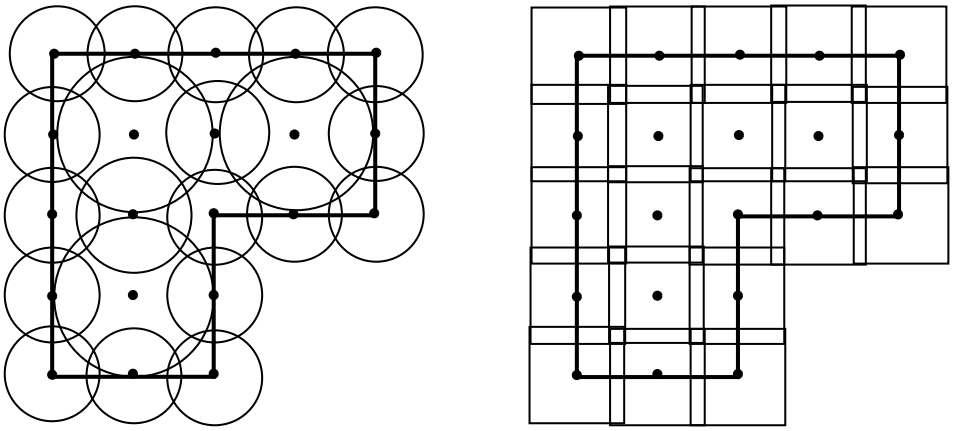

(a) Open covering build using circles.

(b) Open covering build using rectangles.

Figure 1: Examples of open coverings that can be used in the *hp* cloud method.

are global basis functions that possesses the following properties

$$\textbf{1)}\ \ \varphi_\alpha \in C_0^s(\omega_\alpha),\ s \geq 0, \qquad 1 \leq \alpha \leq N$$

$$\textbf{2)}\ \ \sum_{\alpha=1}^{N} \varphi_\alpha(\boldsymbol{x}) = 1, \qquad \forall\, \boldsymbol{x} \in \Omega$$

There is no unique way to build functions φ_α satisfying the above requirements. Each approach has its own merits and embedded costs. The choice of a particular partition of unity should be based on

- the class of problems to be solved, e.g. linear or non-linear problems,
- the complexity of the geometry of the domain,
- the regularity required from the approximation, e.g. C^0, C^1, or higher,
- the importance of the meshless character of the approximation, etc.

Consider, for example, the conventional finite element meshe of triangles and quadrilaterals shown in Fig. 2 on which continuous global Lagrangian basis functions (shape functions) N_α are constructed at each nodal point $\boldsymbol{x}_\alpha$, $\alpha = 1, 2, \ldots, N$. These functions are such that

$$\sum_{\alpha=1}^{N} N_\alpha(\boldsymbol{x}) = 1, \qquad \text{at any } \boldsymbol{x} \in \bar{\Omega}$$

and thus form a partition of unity. By setting $\varphi_\alpha \equiv N_\alpha$, Oden at al. [6] have built cloud-based *hp* finite element approximations using bi-linear finite elements as a partition of unity (see also Section 2.1). In this case, a cloud ω_α is the union of the finite elements sharing a node.

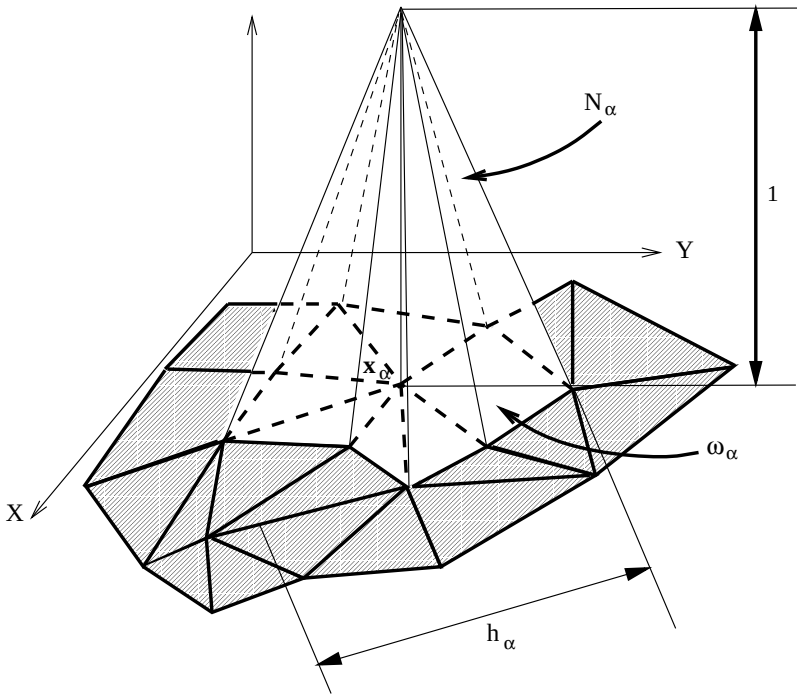

Figure 2: Global finite element shape function N_α built on a mesh of triangles and quadrilaterals.

Another example of a partition of unity are the so called Shepard functions [8]. This partition of unity can be built as follows

Let $\mathcal{W}_\alpha : \mathbb{R}^n \to \mathbb{R}$ denote a *weighting function* with compact support ω_α that belongs to the space $C_0^s(\omega_\alpha)$, $s \geq 0$ and suppose that

$$\mathcal{W}_\alpha(\boldsymbol{x}) \geq 0 \qquad \forall\ \boldsymbol{x}\ \in \Omega$$

In the case of the clouds defined by

$$\omega_\alpha := \{\boldsymbol{y} \in \mathbb{R}^n |\ \|\boldsymbol{x}_\alpha - \boldsymbol{y}\|_{\mathbb{R}^n} < h_\alpha\} \tag{2}$$

weighting functions $\mathcal{W}_\alpha$ can be implemented with any degree of regularity using "ridge" functions. More specifically, the weighting functions $\mathcal{W}_\alpha$ can be implemented through the composition

$$\mathcal{W}_\alpha(\boldsymbol{x}) := g(r_\alpha)$$

where g is, e.g., a B-spline with compact support $[-1,1]$ and r_α is the functional

$$r_\alpha := \frac{\|\boldsymbol{x} - \boldsymbol{x}_\alpha\|_{I\!R^n}}{h_\alpha}$$

Details on the construction of the B-splines can be found in, e.g., [1]. A similar technique can be used to build weighting functions on clouds that are convex sets.

The partition of unity functions φ_α can then be defined by

$$\boxed{\varphi_\alpha(\boldsymbol{x}) = \frac{\mathcal{W}_\alpha(\boldsymbol{x})}{\sum_\beta \mathcal{W}_\beta(\boldsymbol{x})} \qquad \beta \in \{\gamma : \mathcal{W}_\gamma(\boldsymbol{x}) \neq 0\}} \tag{3}$$

which are known as Shepard functions [8]. The main advantages of this particular partition of unity are

- it is meshless—there is no need to partition the domain to build this kind of partition of unity,
- it can easily be implemented in any dimension,
- it can be constructed with any degree of regularity
- it allows easy implementation of h adaptivity, as demonstrated in [3].

2.1 The Family of Cloud Functions $\mathcal{F}_N^p$

The basic idea used to construct the *hp* clouds functions is very simple although not so intuitive. The *hp* cloud functions are constructed by multiplying a partition of unity by functions that have good approximating properties, e.g. polynomials, harmonic functions, etc. It should be emphasized that any partition of unity can be used to build the *hp* cloud functions.

Let $\widehat{\mathcal{L}}_p := \left\{\widehat{L}_i\right\}_{i\in\mathcal{I}}$, denote a set of functions $\widehat{L}_i$ defined on the unit circle

$$\widehat{\omega} := \{\boldsymbol{\xi} \in I\!R^n |\ \|\boldsymbol{\xi}\|_{I\!R^n} < 1\}$$

satisfying

$$\mathcal{P}_p(\widehat{\omega}) \subset \text{span}(\widehat{\mathcal{L}}_p) \tag{4}$$

In the above, $\mathcal{I}$ denotes an index set and $\mathcal{P}_p$ the space of polynomials of degree less than or equal to p. The functions $\widehat{L}_i$ are denoted *higher order basis functions*.

The family of *hp* cloud functions $\mathcal{F}_N^p$ is defined by

$$\mathcal{F}_N^p := \bigcup_{\alpha=1}^{N} \mathcal{N}_\alpha^p, \qquad \mathcal{N}_\alpha^p = \{\ \varphi_\alpha(\boldsymbol{x}) L_{i\alpha}(\boldsymbol{x}) :\ i \in \mathcal{I}\ \} \tag{5}$$

where N is the number of nodes in the domain and

$$L_{i\alpha}(\boldsymbol{x}) = \widehat{L}_i \circ \mathbf{F}_\alpha^{-1}(\boldsymbol{x}) \tag{6}$$

$$\mathbf{F}_\alpha^{-1} : \omega_\alpha \to \widehat{\omega}, \qquad \mathbf{F}_\alpha^{-1}(\boldsymbol{x}) := \frac{\boldsymbol{x} - \boldsymbol{x}_\alpha}{h_\alpha} \tag{7}$$

According to the above definition, $\mathcal{F}_N^p$ is constructed by multiplying each partition of unity function φ_α by the elements from the set $\widehat{\mathcal{L}}_p$ (higher order basis functions). One element from the space of *hp* cloud functions can be written as

$$u^{hp}(\boldsymbol{x}) = \sum_{\alpha=1}^{N} \sum_{i \in \mathcal{I}} a_{\alpha i} \left(\varphi_\alpha(\boldsymbol{x}) L_{i\alpha}(\boldsymbol{x}) \right)$$

The following theorems are proved in [4].

Theorem 2.1 *Let $\mathcal{L}_p := \{L_i\}_{i \in \mathcal{I}}$ and L_i be the same functions $\widehat{L}_i$ but defined on Ω. Then $\mathcal{L}_p \subset span\{\mathcal{F}_N^p\}$.*

Corollary 2.1 *Let $\mathcal{P}_p(\Omega)$ be the space of polynomials of degree less than or equal to p defined on Ω. Then $\mathcal{P}_p(\Omega) \subset span\,\{\mathcal{F}_N^p\}$.*

Therefore, the elements from the set $\mathcal{L}_p$ can be recovered through linear combinations of the *hp* clouds functions. This is one of the most fundamental properties of the *hp* cloud functions.

Figure 3(a) shows the Shepard partition of unity function φ_α associated with a node $\boldsymbol{x}_\alpha$ at the origin of the domain $\Omega = (-1,1) \times (-1,1)$. A uniform 5×5 node arrangement and quartic splines are used to build it. Figure 3(b) shows the function $y\varphi_\alpha$ from the families $\mathcal{F}_{N=25}^{p \geq 1}$.

As mentioned above, finite elements can be used as a partition of unity to build cloud functions. Figure 4(a) shows a bilinear global finite element shape function N_α associated with a node from the mesh shown in Fig. 12. Figure 4(b) shows the cloud function $y^2 N_\alpha$.

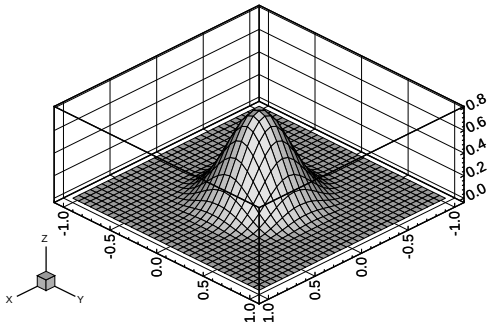

(a) 2-D partition of unity function φ_α.

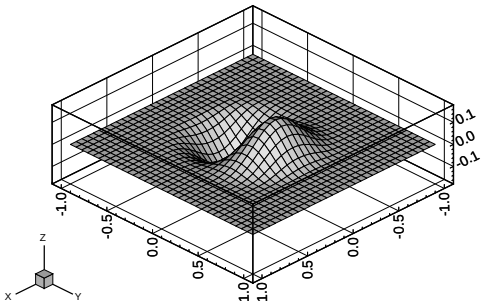

(b) 2-D *hp* cloud function $y\varphi_\alpha$ from the families $\mathcal{F}^{p\geq 1}_{N=25}$.

Figure 3: 2-D *hp* cloud functions built using a meshless partition of unity.

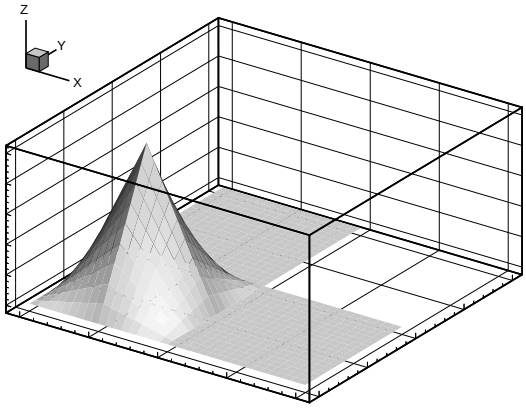

(a) Bi-linear shape function (partition of unity function).

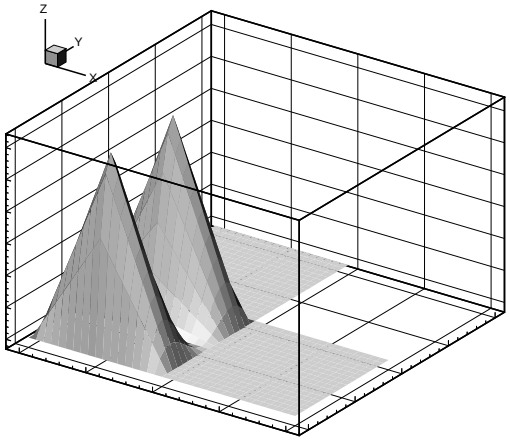

(b) Higher order hierarchical shape function built from the product of the bilinear shape function shown in (a) and the monomial y^2.

Figure 4: 2-D *hp* cloud functions built using a finite element partition of unity.

2.1.1 The Use of Customized Functions

There are several situations in which the inclusion in the set $\widehat{\mathcal{L}}_p$ of specially customized functions to model, e.g., boundary layers, shocks, singularities, etc., can be very advantageous. This is the case in the stress analysis of cracks where the quantities of interest are the stress intensity factors. Oden and Duarte [7] have demonstrated that the amplitude of any number of stress intensity factors can be obtained from the coefficients of customized *hp* cloud functions without any additional work. We summarize bellow the main results of Oden and Duarte [7].

Assuming traction-free crack surfaces and no body forces, the displacement vector $\boldsymbol{u} = \{u_\xi, u_\eta\}^T$ in the neighborhood of a crack can be written [9,10]

$$\boldsymbol{u}(r,\theta) = \left\{ \begin{array}{c} u_\xi(r,\theta) \\ u_\eta(r,\theta) \end{array} \right\} = \sum_{j=1}^{M} \left[A_j^{(1)} \left\{ \begin{array}{c} u_{\xi j}^{(1)}(r,\theta) \\ u_{\eta j}^{(1)}(r,\theta) \end{array} \right\} + A_j^{(2)} \left\{ \begin{array}{c} u_{\xi j}^{(2)}(r,\theta) \\ u_{\eta j}^{(2)}(r,\theta) \end{array} \right\} \right] + + \left\{ \begin{array}{c} \underline{u}_\xi(r,\theta) \\ \underline{u}_\eta(r,\theta) \end{array} \right\} \tag{8}$$

where (r,θ) are the polar coordinates relative to an origin at the crack tip (cf. Fig. 5), $u_{\xi j}^{(1)}$, $u_{\eta j}^{(1)}$, $u_{\xi j}^{(2)}$, $u_{\eta j}^{(2)}$ are Cartesian components of $\boldsymbol{u}$ in the $\xi-$ and $\eta-$ directions, $\underline{u}_\xi(r,\theta)$ and $\underline{u}_\eta(r,\theta)$ are functions smoother than any term in the sum. The coefficients $A_j^{(1)}$, $A_j^{(2)}$ are called generalized stress intensity factors.

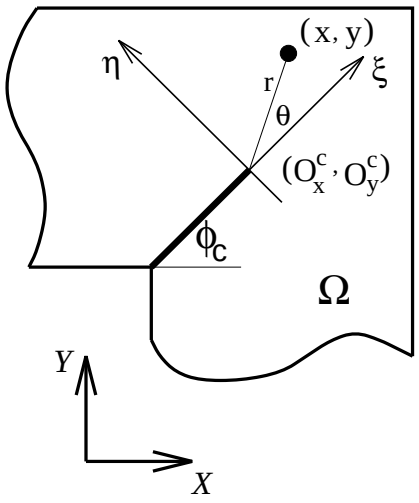

Figure 5: Coordinate systems associated with the crack tip.

The singular *hp* cloud functions associated with a cloud ω_β, $\beta \in \mathcal{I}_c$, are defined by

$$\mathcal{C}_\beta^M := \left\{ \varphi_\beta \left[u_{xj}^{(1)},\ u_{xj}^{(2)},\ u_{yj}^{(1)},\ u_{yj}^{(2)} \right] \mid\ j = 1, \ldots, M \right\} \tag{9}$$

The cloud ω_β is said to be an *enriched cloud*. The functions $u_{xj}^{(1)},\ u_{xj}^{(2)},\ u_{yj}^{(1)},\ u_{yj}^{(2)}$ are the same as in (8) but transformed to the physical coordinates (x, y). Here, $\mathcal{I}_c$ denotes the index set of the clouds that include in their local spaces the near crack expansion.

The *enriched hp cloud functions* is then defined by

$$\boxed{\mathcal{F}_N^{p,\text{crack}} := \left\{ \left[\bigcup_{\alpha=1}^{N} \mathcal{N}_\alpha^p \right] \bigcup \left[\bigcup_{\beta \in \mathcal{I}_c} \mathcal{C}_\beta^M \right] \right\}} \tag{10}$$

Where $\mathcal{N}_\alpha^p$ is defined in (5). Note that all elements from $\mathcal{F}_N^{p,\text{crack}}$ have compact support. The main advantage of using the enriched clouds as defined above is that the amplitude of any number of stress intensity factors can be obtained from the coefficients of these functions [7]. This technique is demonstrated numerically in the next section.

3 Numerical Experiments

In this section two boundary-value problems are solved using *hp* cloud approximations and the Galerkin method. Details on the implementation of domain and boundary integration can be found in [3, 5]. In the first numerical experiment, the *hp* cloud functions are built using the meshless partition of unity defined in (3). This experiment demonstrates how the use of customized functions, made possible by the *hp* cloud method, can lead to exponential convergence of the solution even in the presence of singularities and without using strongly graded meshes as required in traditional *hp* finite elements methods.

In the second experiment the partition of unity is composed of global finite element shape functions. This experiment demonstrates how non-uniform *hp* distributions can be constructed quite naturally within the *hp* cloud framework.

3.1 An Inclined Crack Problem

The cracked panel shown in Fig. 6 is analyzed using the enriched *hp* cloud functions defined in (10). The *hp* cloud results are compared with those presented by Szabó and Babuška [9] for the *p* version of the finite element method. In this problem, both the symmetric and anti-symmetric part of the expansion (8) are non-zero.

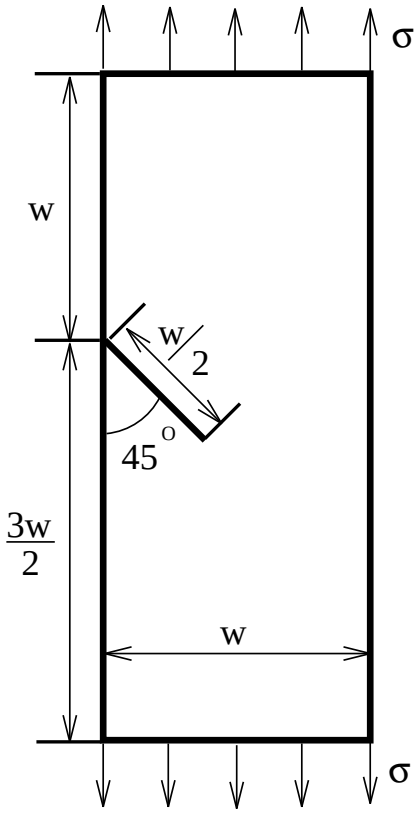

Figure 6: Problem definition.

The plane stress condition, a Poisson's ratio of 0.3 and unit thickness are assumed. In addition we adopt $E = 1$, w $= 1$ and $\sigma = 1$ (cf. Fig. 6).

The *hp* cloud discretization is depicted in Fig. 7(a). There are only $N = 9$ clouds. Note that no special nodal arrangement is used near the singularity at the crack tip. The cloud at the crack tip, denoted by ω_{tip}, is the only enriched cloud. All other clouds have only polynomials in their local spaces. The *hp* cloud space is given by

$$\mathcal{F}^{p,\text{crack}}_{N=9} = \left\{ \Big[\bigcup_{\alpha=1,\ \alpha\neq tip}^{N} \mathcal{N}^p_\alpha \Big] \cup \Big[\mathcal{N}^1_{\alpha=tip} \cup \mathcal{C}^M_{\alpha=tip} \Big] \right\} \tag{11}$$

where $M = 3 + 5(p-1)$.

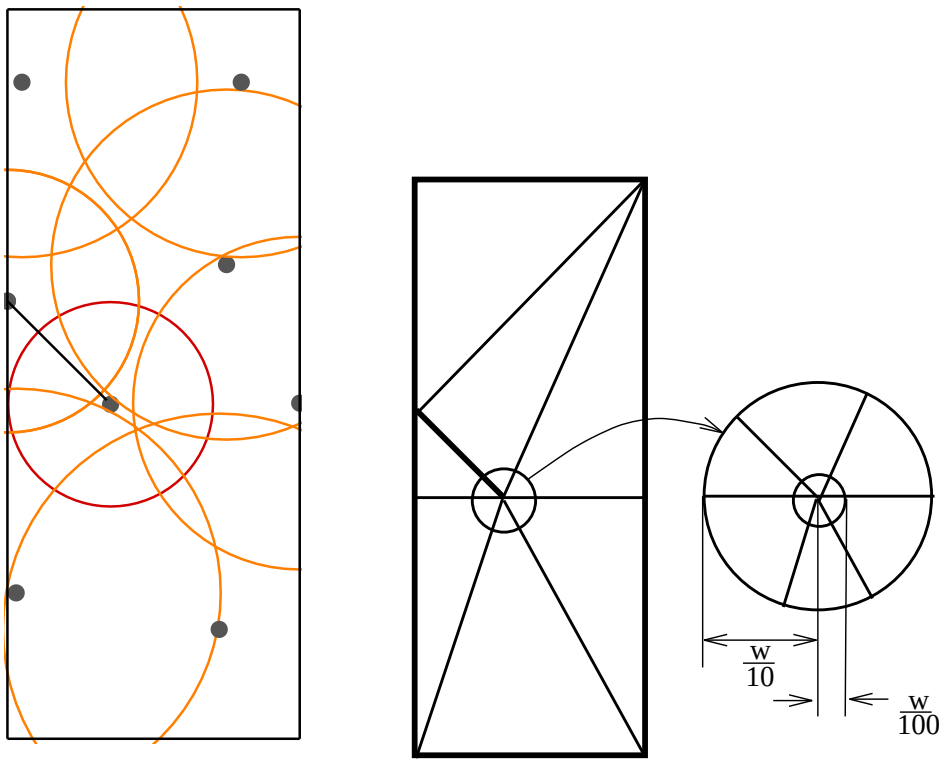

(a) *hp* cloud discretization.

(b) Finite element discretization.

Figure 7: *hp* cloud and finite element discretizations.

Figure 7(b) shows the finite element mesh used by Szabó and Babuška [9]. Three layers of finite elements are used around the crack tip.

The stress intensity factors K_I and K_{II} are normalized as follows

$$\tilde{K}_I := \frac{K_I}{\sigma\sqrt{2\pi \mathrm{w}}} \qquad \tilde{K}_{II} := \frac{K_{II}}{\sigma\sqrt{2\pi \mathrm{w}}}$$

Figures 8 and 9 show the *hp* cloud results. The values obtained using the p version of the finite element method with the cutoff function method (CFM) and the contour integral method (CIM) [9] are also shown in Figs. 8 and 9. The three techniques converge to the same values but the *hp* cloud method requires fewer degrees of freedom than the finite element method with the CFM or the CIM. The results are also shown in Tables 1 and 2 for the *hp* cloud method and the finite element method, respectively. Figures 10(a) and (b) show the computed stress components σ_{11} and σ_{12}, respectively. The plots are in the (θ, r) plane. Figure 10(c) depicts the component u_1 of the displacement vector in the (x, y) plane.

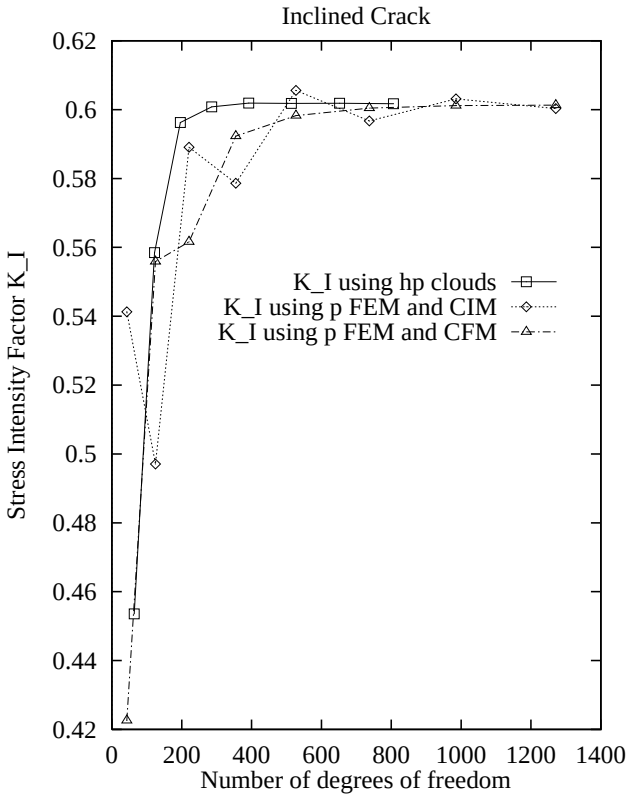

Figure 8: Convergence of $\tilde{K}_I$.

Table 1: Values of $\tilde{K}_I$, $\tilde{K}_{II}$ and strain energy for the inclined crack computed using *hp* clouds.

Step	N	$\tilde{K}_I$	$\tilde{K}_{II}$	U_{hp}
1	64	0.453 551 548 01	-0.273 638 260 31	1.566 046 631 087
2	122	0.558 479 531 07	-0.297 078 107 32	1.662 449 370 686
3	196	0.596 284 457 14	-0.290 000 508 19	1.697 944 565 848
4	286	0.600 795 484 57	-0.290 340 435 49	1.703 163 179 320
5	392	0.601 886 119 14	-0.290 770 762 20	1.703 796 511 631
6	514	0.601 821 961 72	-0.290 837 611 07	1.703 975 037 245
7	652	0.601 853 671 45	-0.290 943 515 98	1.704 016 285 211
8	806	0.601 718 130 52	-0.291 110 545 79	1.704 022 915 131

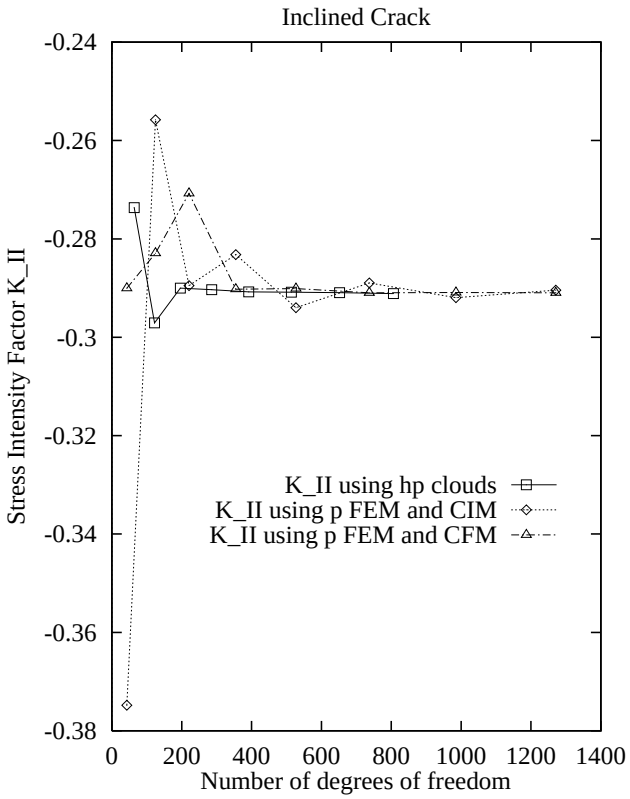

Figure 9: Convergence of $\tilde{K}_{II}$.

Table 2: Values of $\tilde{K}_I$ and $\tilde{K}_{II}$ for the inclined crack computed using p fem with CFM and CIM [9].

p	N	$\tilde{K}_I$(CIM)	$\tilde{K}_I$(CFM)	$\tilde{K}_{II}(CIF)$	$\tilde{K}_{II}$(CFM)
1	43	0.541 27	0.422 59	-0.374 80	-0.290 05
2	125	0.497 08	0.555 88	-0.255 78	-0.282 92
3	221	0.589 09	0.561 61	-0.289 51	-0.270 74
4	355	0.578 64	0.592 32	-0.283 19	-0.290 22
5	527	0.605 58	0.598 25	-0.293 98	-0.290 12
6	737	0.596 72	0.600 43	-0.288 97	-0.290 97
7	985	0.603 13	0.601 19	-0.291 96	-0.290 91
8	1271	0.600 32	0.601 32	-0.290 42	-0.290 95

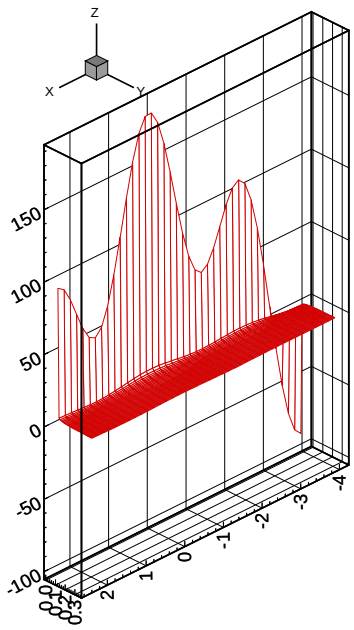

(a) σ_{11} in the (θ, r) plane.

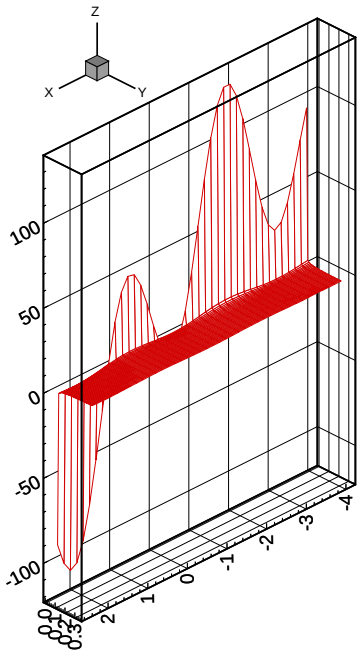

(b) σ_{12} in the (θ, r) plane.

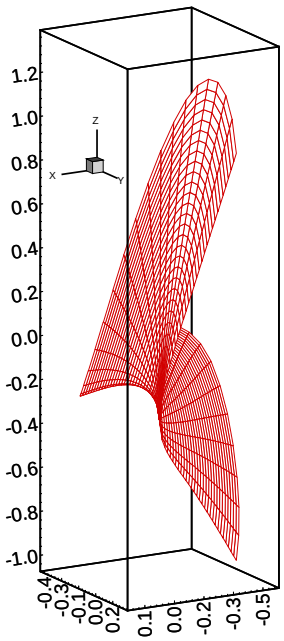

(c) u_1.

Figure 10: σ_{11} and σ_{12} in the (θ, r) plane and u_1 in the (x, y) plane.

3.2 *hp* Adaptivity Using an Hybrid FE/Cloud Approximation

We shall now consider the problem of an L-shaped plane elastic body loaded by the tractions associated with the following stress field

$$\begin{aligned}
\sigma_{xx}(r,\theta) &= \lambda r^{\lambda-1}[(2-Q(\lambda+1))\cos(\lambda-1)\theta-(\lambda-1)\cos(\lambda-3)\theta] \\
\sigma_{yy}(r,\theta) &= \lambda r^{\lambda-1}[(2+Q(\lambda+1))\cos(\lambda-1)\theta+(\lambda-1)\cos(\lambda-3)\theta] \qquad (12)\\
\sigma_{xy}(r,\theta) &= \lambda r^{\lambda-1}[(\lambda-1)\sin(\lambda-3)\theta+Q(\lambda+1)\sin(\lambda-1)\theta]
\end{aligned}$$

where (r,θ) is the polar coordinate system shown in Fig. 11, $\lambda = 0.544\,483\,737$, $Q = 0.543\,075\,579$.

The stress field (12) corresponds to the first term of the symmetric part of the expansion of the elasticity solution in the neighborhood of the corner A shown in Fig. 11 [9].

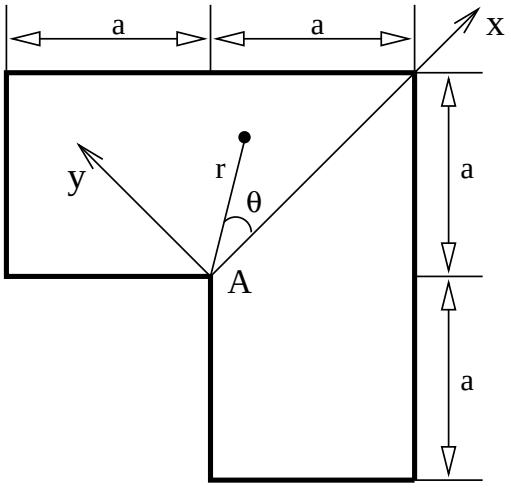

Figure 11: L-shaped elastic body.

Plane strain conditions, unity thickness and Poisson's ratio of 0.3 are assumed. The strain energy of the exact solution is given by [9]

$$\mathcal{E}(u) = 4.154\,544\,23\frac{a^{2\lambda}}{E}$$

where E is the modulus of elasticity and a is the dimension shown in Fig. 11. The values $E = a = 1$ are assumed in the calculations.

Two sequences of discretizations, $\mathcal{S}_1$ and $\mathcal{S}_2$, are used to solve this problem. In the former, the uniform mesh shown in Fig. 12 is used and the polynomial order of the

approximations ranges from 1 to 8. A strongly graded mesh, as shown in Fig. 13, and non-uniform p distributions are used in the second sequence of discretizations. Figures 14 and 15 show the p distribution used in the fourth step of this sequence. The polynomial order of the clouds decrease linearly towards the singularity while the size of the finite elements decrease geometrically. Geometric factors $q = 0.15$ and $q = 0.10$ are used (cf. Fig. 13).

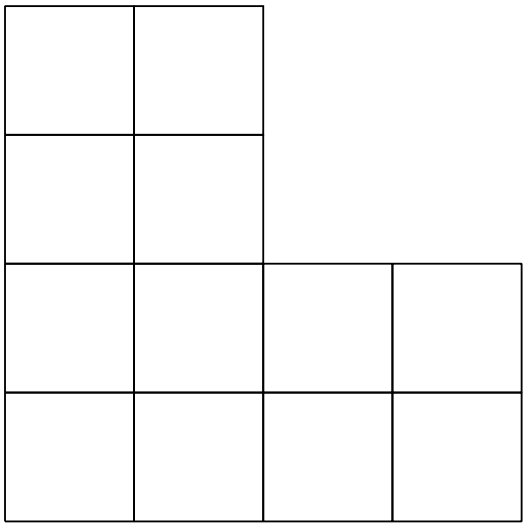

Figure 12: Uniform mesh for the L-shaped body.

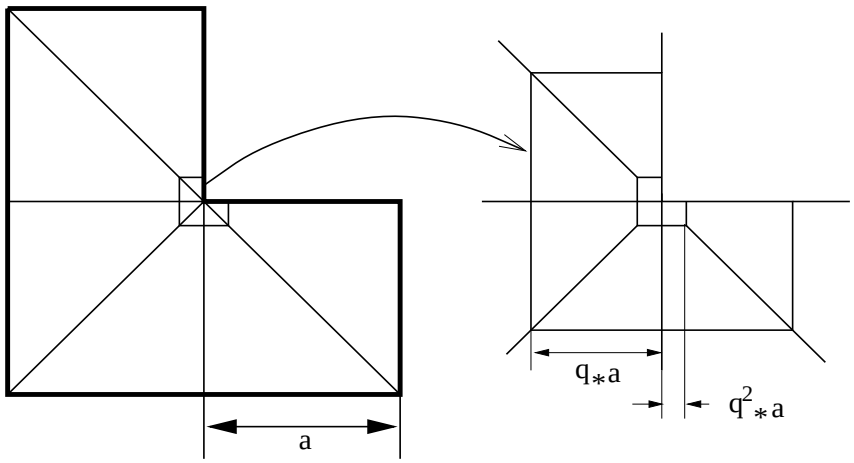

Figure 13: Geometric mesh for the L-shaped body. Geometric factors of $q = 0.15$ and $q = 0.10$ are adopted in the computations.

The relative error, measured in the energy norm, versus the number of degrees of freedom is shown in Fig. 16 for the sequences of discretizations $\mathcal{S}_1$ and $\mathcal{S}_2$ (for $q = 0.15$ and $q = 0.10$). As expected, the uniform mesh gives an algebraic rate of

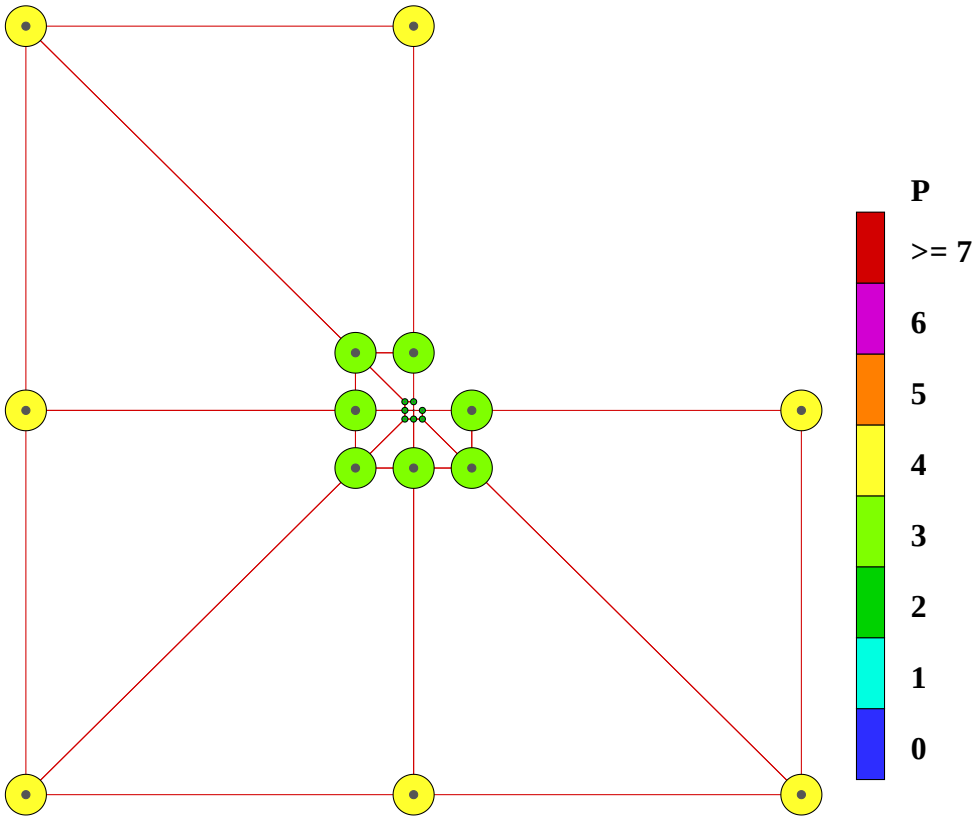

Figure 14: Polynomial order associated with the clouds at the fourth step of the sequence of discretizations $\mathcal{S}_2$.

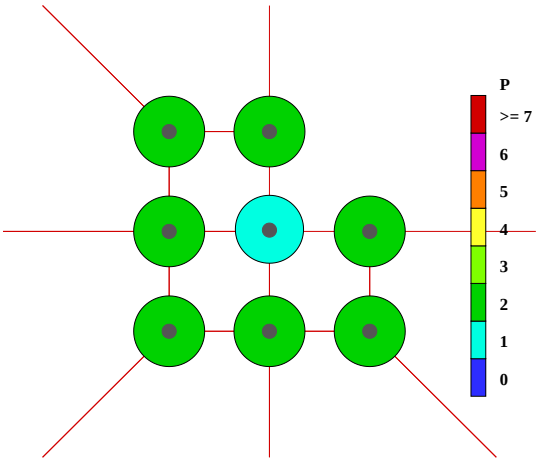

Figure 15: Zoom at clouds near the re-entrant corner of Fig. 14.

convergence while the strongly graded meshes leads to an exponential rate of convergence. This kind of behavior is typical of *hp*- finite element methods. However, the construction of non-uniform *h*- and *p*- discretizations in a cloud based framework is considerably more straightforward than in conventional *hp*- finite element methods. The sequence $\mathcal{S}_2$ with a geometric factor $q = 0.10$ gives better results than the sequence $\mathcal{S}_2$ with $q = 0.15$.

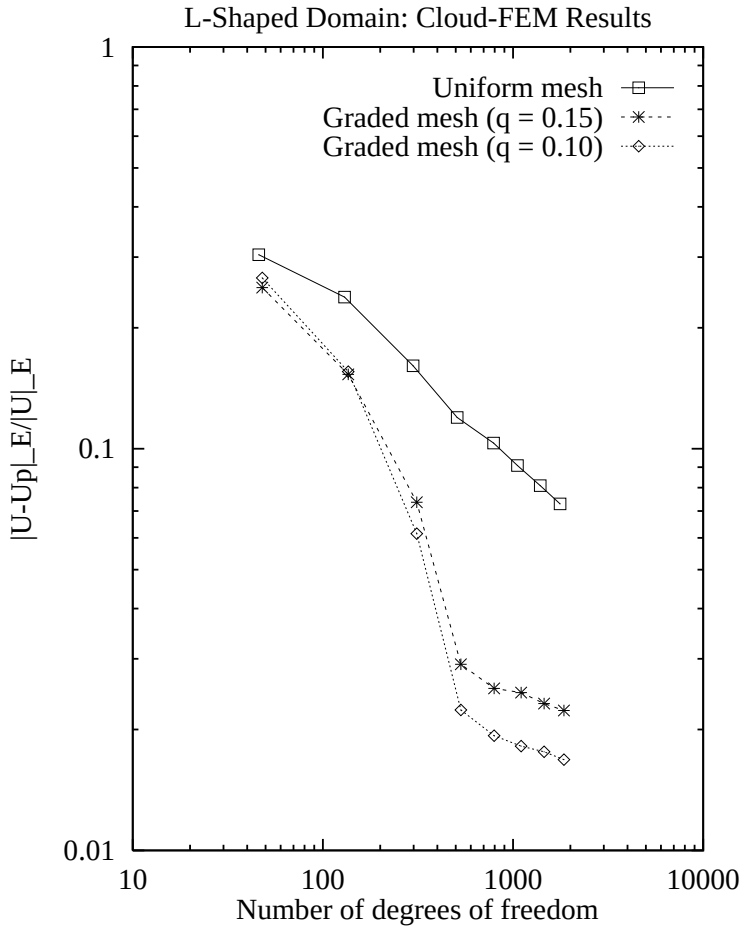

Figure 16: Convergence in the energy norm for uniform and non-uniform cloud-based *hp*- distributions.

4 Conclusions

The *hp* cloud method can be combined with the classical finite element method to produce an effective technique for solving boundary-value problems; alternatively, it can be used with any technique that produces a partition of unity, without traditional meshing considerations. One of the most attractive features of such ap-

proaches is that special customized clouds can be developed which enhance convergence rates and facilitate applications to special problems such as fracture mechanics. When implemented on a FEM generated PU, a nonuniform *hp* finite element method is produced which exhibits exponential convergence rates.

Acknowledgment: The support of this work by the the Army Research Office (J. T. Oden and C. A. Duarte) under contract DAAH04-96-0062 and the CNPq Graduate Fellowship Program (C. A. Duarte) grant # 200498/92-4 are gratefully acknowledged.

References

[1] Carl deBoor. *A Practical Guide to Splines*. Springer-Verlag, New York, 1978.

[2] C. A. M. Duarte and J. T. Oden. Hp clouds–a meshless method to solve boundary-value problems. Technical Report 95-05, TICAM, The University of Texas at Austin, 1995.

[3] C. A. M. Duarte and J. T. Oden. An *hp* adaptive method using clouds. Technical report, TICAM, The University of Texas at Austin, 1996. To appear in *Computer Methods in Applied Mechanics and Engineering*.

[4] C. A. M. Duarte and J. T. Oden. *Hp* clouds—an *hp* meshless method. *Numerical Methods for Partial Differential Equations*, 12:673–705, 1996.

[5] C. Armando Duarte. *The* hp *Cloud Method*. PhD thesis, The University of Texas at Austin, Austin, TX, USA, December 1996.

[6] J. T. Oden, C. A. Duarte, and O. C. Zienkiewicz. A new cloud-based *hp* finite element method. *Computer Methods in Applied Mechanics and Engineering* (to appear).

[7] J. T. Oden and C. A. M. Duarte. Solution of singular problems using *h-p* clouds. In *MAFELAP 96*, 1996.

[8] D. Shepard. A two-dimensional function for irregularly spaced data. In *ACM National Conference*, pages 517–524, 1968.

[9] B. A. Szabo and I. Babuska. Computation of the amplitude of stress singular terms for cracks and reentrant corners. In T. A. Cruse, editor, *Fracture Mechanics: Nineteenth Symposium, ASTM STP 969*, pages 101–124, 1988.

[10] Barna Szabo and Ivo Babuska. *Finite Element Analysis*. John Wiley and Sons, New York, 1991.